ELSEVIER

Coordination Chemistry Reviews
208 (2000) 227–241

COORDINATION CHEMISTRY REVIEWS

www.elsevier.com/locate/ccr

Luminescent homoatomic exciplexes in dicyanoargenate(I) ions doped in alkali halide crystals. 'Exciplex tuning' by site-selective excitation and variation of the dopant concentration

Howard H. Patterson *, Sofian M. Kanan, Mohammad A. Omary

Department of Chemistry, University of Maine, 5706 Aubert Hall, Orono, ME 04469-5706, USA

Received 29 August 1999; received in revised form 15 December 1999; accepted 15 December 1999

Contents

Abstract . . . 227
1. Introduction . . . 228
2. Experimental . . . 229
3. Results and discussion . . . 230
   3.1 Exciplex tuning by site-selective excitation . . . 230
   3.2 Exciplex tuning by variation of the dopant concentration . . . 234
   3.3 Energy transfer between excimers and exciplexes . . . 236
4. Conclusions . . . 239
Acknowledgements . . . 240
References . . . 240

Abstract

The photoluminescence spectra of dicyanoargenate(I) ions doped in KCl host crystals show several ultraviolet and visible emission bands. Each emission band becomes dominant

* Corresponding author. Tel.: +1-207-5811178; fax: +1-207-5811191.
E-mail address: howardp@maine.maine.edu (H.H. Patterson).

PII: S0010-8545(00)00294-0

at a characteristic excitation wavelength; i.e. the energy of the emission can be tuned. Both the experimental and theoretical results suggest the formation of Ag–Ag bonded excimers and exciplexes between adjacent $Ag(CN)_2^-$ ions in the host lattice. The experimental evidence includes the broadness, the absence of detailed structure, and the low band energies of the luminescent bands. Ab-initio and extended Hückel calculations show that the lowest unoccupied molecular orbital (LUMO) is bonding with respect to Ag–Ag bonds while the highest occupied molecular orbital (HOMO) is antibonding. Further, the calculations indicate the existence of exciplexes with shorter Ag–Ag bond distances, higher binding energies, and larger Ag–Ag overlap populations than the corresponding ground state oligomers. The results in this study give rise to a new optical phenomenon which is called 'exciplex tuning'. Tuning of the emission over the 285–610 nm wavelength range has been achieved in $KCl/Ag(CN)_2^-$ crystals by site-selective excitation and varying the $Ag(CN)_2^-$ dopant concentration.

Keywords: Exciplex; Excimer; Luminescence; Silver–silver interactions; HOMO-LUMO

1. Introduction

The photophysical properties of coordination compounds of the d^{10} monovalent ions of the coinage metals continue to receive much attention. For instance, coordination compounds of Cu(I) have been extensively studied and investigated for their structural and spectral properties [1–4]. Similarly, interest in gold(I) compounds has been increasing in recent years partially because of the tremendous attention given to the relation between the electronic properties of gold(I) compounds and the so called aurophilic attraction [5], namely ground state Au–Au interactions. By contrast, coordination compounds of Ag(I) have received very little attention. Most of the attention given to Ag(I) compounds has been concentrated on photophysical and photochemical studies of simple silver halides due to their applications in photographic materials and optical fibers [6,7]. Recently, analogous argentophilic attraction has been found in Ag(I) coordination compounds [8,9]. This discovery has led to further photophysical studies of Ag(I) doped alkali halide crystals in order to probe argentophilic attraction in the ground and excited electronic states.

Exciplex formation is well known in organic compounds [10–12] but less common in inorganic compounds [13]. Photoluminescence studies of dicyanoargenate(I) species have shown that Ag–Ag interactions are much stronger in the lowest electronic excited state than in the ground state. For example, the photoluminescence behavior of single crystals of $TlAg(CN)_2$ have been studied as a function of temperature [14]. The results correlate with the crystal structure of the compound which indicates the presence of two environments with silver–silver interactions [8]. This is the first example of exciplex formation between silver ions in the solid state for coordination compounds.

Recently, we have discovered a new class of inorganic excimers and exciplexes in $Ag(CN)_2^-$ doped in KCl [15,16] and NaCl [17] host systems in which the bonding

occurs between the same type of metal atoms. $*[Ag(CN)_2^-]_n$ are the first reported homoatomic metal–metal bonded exciplexes in coordination compounds. The emission in the $Ag(CN)_2^-$/KCl system results from silver–silver bonded excimers and exciplexes with a formula of $*[Ag(CN)_2^-]_n$. In this review an excited state dimer is referred to as an 'excimer' while excited state trimers and longer oligomers are called 'exciplexes'. The luminescence is tuned by selecting the excitation wavelength characteristic of each $*[Ag(CN)_2^-]_n$ emissive exciplex or by varying the dopant concentration. A kinetic model is presented to explain the energy transfer pathways between various emitting centers in the mixed crystals.

2. Experimental

Crystals were grown by slow evaporation of aqueous solutions containing 2 M KCl and 0.05 M $K^+[Ag(CN)_2^-]$. By harvesting samples at different stages during the evaporation, doped crystals of KCl with different $[Ag(CN)_2^-]$ contents were obtained.

The silver content was determined by atomic absorption spectroscopy using a Varian Spectra AA-20 spectrophotometer with an air-acetylene flame and an Ag analytical lamp operating at 328 nm.

Photoluminescence spectra were recorded with a model QuantaMaster-1046 fluorescence spectrophotometer from Photon Technology International, PTI. The instrument is equipped with two excitation monochromators and a 75-W xenon lamp. All luminescence spectra were recorded at liquid nitrogen temperature for a single crystal using a Model LT-3-110 Heli-Tran cryogenic liquid transfer system. Correction of the excitation spectra for spectral variation in the lamp intensity was carried out using the quantum counter rhodamine B. Life-time and time-resolved measurements were carried out with a Laser Strobe system from PTI equipped with a nitrogen laser, a dye laser, a frequency doubler, and a gated microsecond detector for the microsecond time domain. Some measurements were also carried out with a QuantaMaster-2 system utilizing a microsecond Xe-flash lamp and a gated microsecond detector.

Fourier transform infrared (FTIR) spectra were obtained using a Bio-Rad Digilab FTS-60 spectrometer equipped with a setup which allows for measuring the FTIR spectra of a single crystal using the reflectance mode. A gold-plated metal plate was used as a reference for the reflectance spectra. The crystals were aligned visually using a microscope prior to the acquisition of the infrared spectra.

Extended Hückel molecular orbital calculations were carried out using the FORTICON8 program (QCMP011). This program allows for excited-state calculations. The calculations were carried out for a monomer, dimer, and trimer of $Ag(CN)_2^-$ in a KCl crystal lattice as well as isolated ions. Restricted Hartree–Fock ab-initio calculations were carried out using the STO-3G basis set available in SPARTAN (Version 4.1.1, Wavefunction, Irvine, CA) to generate the highest occupied molecular orbital (HOMO) and lowest unoccupied molecular orbital (LUMO) surfaces of $[Ag(CN)_2^-]_n$ oligomers.

3. Results and discussion

3.1. Exciplex tuning by site-selective excitation

Atomic absorption analysis of the studied KCl mixed crystals gave a silver content of 1.62% (by weight). Single crystals of $Ag(CN)_2^-$/KCl have photoluminescence spectra that strongly depend on the excitation wavelength. Fig. 1 shows the emission spectra of $Ag(CN)_2^-$/KCl at 77 K as a function of excitation wavelength. Five emission bands at ca. 295, 327, 345, 417 and 548 nm are observed. These bands are labeled as A, B, C, and D as indicated in Fig. 1. The emission bands at 327 and 345 nm overlap with each other so they are given the same label (B). A non-luminescent property of the $Ag(CN)_2^-$ monomer causes all dicyanoargenate(I) emission bands to be a result of silver–silver interactions [15,16]. The emission bands indicate the presence of different aggregations of the $Ag(CN)_2^-$ ions in the KCl lattice. The high-energy band A is assigned to $[Ag(CN)_2^-]_2$ excimers. Bands B and C are assigned to $*[Ag(CN)_2^-]_3$ localized exciplexes. By contrast, the high-energy band D are assigned to $*[Ag(CN)_2^-]_n$ delocalized exciplexes.

Fig. 2 shows the excitation spectra of $Ag(CN)_2^-$/KCl monitoring each of the emission bands A–D. As illustrated in Fig. 2, each emission band is associated with a different excitation peak. A dilute aqueous solution of $Ag(CN)_2^-$ showed one

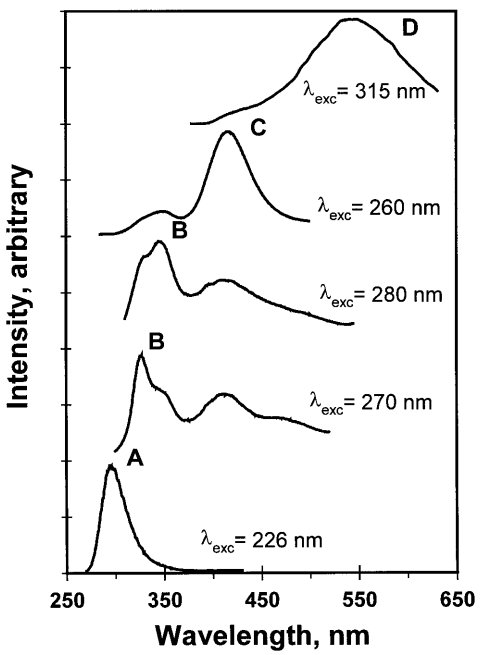

Fig. 1. Exciplex tuning by site-selective excitation: emission spectra of a $[Ag(CN)_2^-]$/KCl crystal at 77 K with different excitation wavelengths. Intensities are not comparable between different spectra.

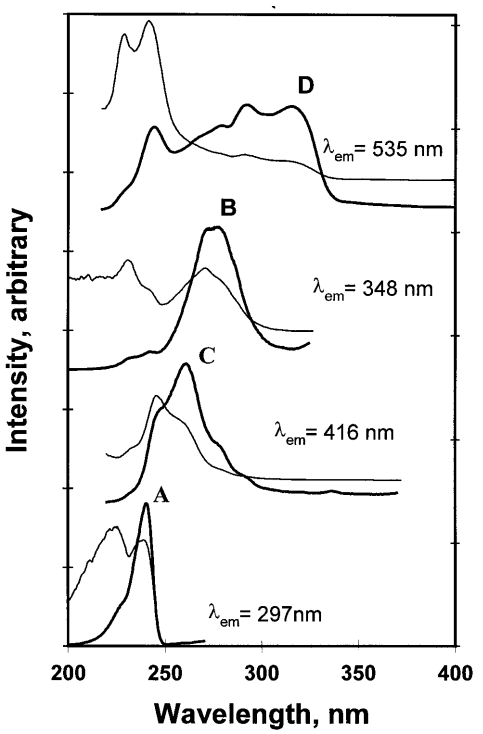

Fig. 2. Corrected (thin lines) and uncorrected (thick lines) excitation spectra of a $[Ag(CN)_2^-]$/KCl crystal at 77 K monitoring the emissions at wavelengths corresponding to the emission maxima of bands A–D in Fig. 1. Intensities are not comparable between different spectra.

absorption band at 196 nm which has been assigned to a charge transfer transition from the d^{10} orbitals of Ag(I) to an empty π^* orbitals of CN^- [18]. The excitation bands of $Ag(CN)_2^-$ /KCl shown in Fig. 2 are red-shifted from the absorption band energy of aqueous $Ag(CN)_2^-$. This red shift is due to silver–silver interactions. The assignment of the luminescence bands of $[Ag(CN)_2^-]$/KCl systems is summarized in Table 1 [15].

The luminescence data suggest that silver–silver interactions are responsible for the luminescence properties of $Ag(CN)_2^-$/KCl. Extended Hückel and ab-initio

Table 1
Assignement of the luminescence bands of $[Ag(CN)_2^-]$/KCl crystals

Band	λ_{max}^{em} (nm)	λ_{max}^{exc} (nm)	Assignment
A	285–300	225–250	$*[Ag(CN)_2^-]_2$ (excimer)
B	310–360	270–290	*cis*-$*[Ag(CN)_2^-]_3$ (localized exciplex)
C	390–430	250–270	*trans*-$*[Ag(CN)_2^-]_3$ (localized exciplex)
D	490–530	300–360	$*[Ag(CN)_2^-]_n$ (delocalized exciplexes)

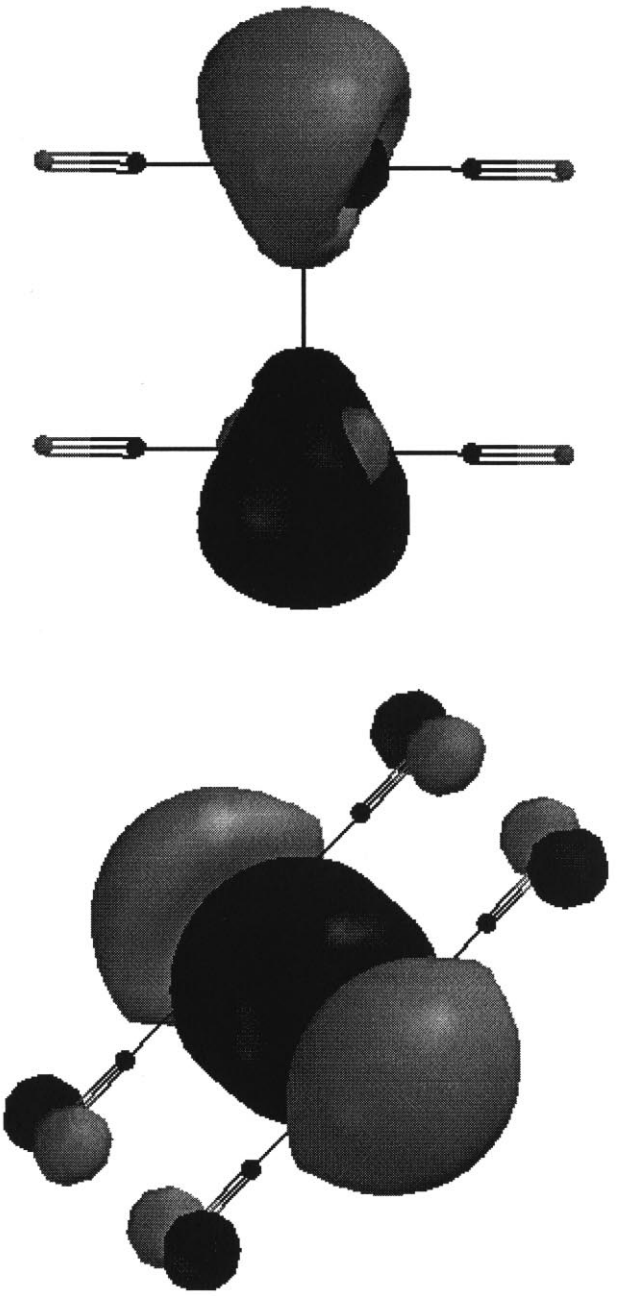

Fig. 3. Surfaces of the highest occupied molecular orbital (HOMO) (top) and lowest unoccupied molecular orbital (LUMO) (bottom) of $[Ag(CN)_2^-]_2$ (eclipsed configuration) as plotted from Hartree–Fock ab initio calculations.

calculations were carried out for the monomer and the eclipsed form of both the dimer and the trimer representations of $Ag(CN)_2^-$/KCl. Frontier orbital Hückel calculations indicate that the HOMO-LUMO gap decreases in the direction of monomer → dimer → trimer. However, the decrease in the HOMO-LUMO gap is very small and cannot explain the low energies of the luminescence bands in Figs. 1 and 2. Since the Ag–Ag separation of 4.5 Å is relatively larger than the summed van der Waals radii of two silver atoms (3.4 Å), ground state Ag–Ag interactions are too weak to cause the low energies of the luminescence bands of the title compound. Therefore, excited state Ag–Ag interactions appear to be responsible for the rather low energy luminescence peaks of $Ag(CN)_2^-$/KCl shown in Figs. 1 and 2.

To test the possibility of excited-state Ag–Ag interactions, both ab-initio and extended Hückel calculations for $[Ag(CN)_2^-]_n$, $n = 1, 2, 3$ have been carried out. Both methods suggest exciplex formation in the $[Ag(CN)_2^-]_n$ model. Ab-initio studies for all aggregations of $Ag(CN)_2^-$ show that the HOMO has Ag–Ag antibonding character, while the LUMO has Ag–Ag bonding character. Fig. 3 shows the surfaces of the HOMO and LUMO of $[Ag(CN)_2^-]_2$ as plotted from Hartree–Fock ab initio calculations and illustrates the Ag–Ag antibonding character of the HOMO and the Ag–Ag bonding character of the LUMO of $[Ag(CN)_2^-]_2$.

Extended Hückel calculations have been carried out to determine potential energy curves for the dimer and trimer forms of $[Ag(CN)_2^-]$. Fig. 4 shows the potential energy curve for the ground and excited states of $[Ag(CN)_2^-]_2$ (eclipsed form). The following results indicate the formation of a $*[Ag(CN)_2^-]_2$ excimer. In comparison with the ground state, the Ag–Ag bond separation is shorter in the first

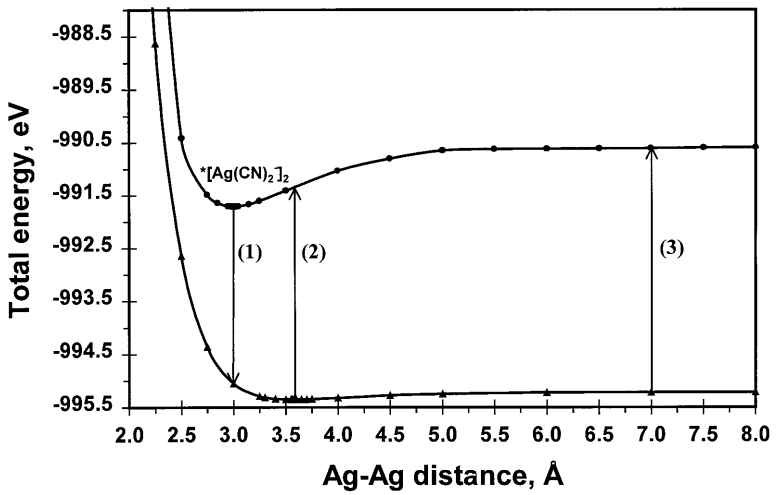

Fig. 4. Excimer emission: potential energy diagram for the ground and the lowest excited state of $[Ag(CN)_2^-]_2$ (eclipsed configuration) plotted from extended Hückel calculations. The excimer $*[Ag(CN)_2^-]_2$ corresponds to the potential minimum of the excited state. Optical transitions shown are: (1) excimer emission; (2) solid-state excitation; and (3) solution absorption.

electronic excited state, the Ag–Ag overlap population is ten times greater in the excited state, and the potential well along the Ag–Ag bond is much deeper in the excited state. Similar trends have been observed for staggered $[Ag(CN)_2^-]_2$ and for both eclipsed and staggered $[Ag(CN)_2^-]_3$. The extremely low energies of the excimer emissions are due to a combined effect of excited-state stabilization and ground state destabilization, as illustrated in Fig. 4.

The luminescence energy can be tuned to a certain value by selecting the characteristic excitation wavelength of the exciplex responsible for this luminescence. Fig. 4 illustrates the optical transitions observed in excimer emission. The excimer emission (transition '1') is depicted as a vertical transition from the minimum of the excited state potential well to the ground state. This transition corresponds to the emission peak labeled A in Fig. 1. Solid-state excitation is depicted as a vertical transition from the minimum of the ground state potential well to the first electronic excited state (transition '2'). There is significant stabilization, especially in the excited state due to Ag–Ag bonding. This stabilization is consistent with the low energies of the excitation bands shown in Fig. 2. Moreover, transition '3' is depicted as a transition from the ground state to the excited state at a long Ag–Ag distance at which no stabilization is present due to Ag–Ag interactions. Transition 3 corresponds to the high energy absorption band at 196 nm of a dilute aqueous solution of $Ag(CN)_2^-$. Similar calculations for $[Ag(CN)_2^-]_3$ have shown lower energies for transitions '1' and '2'.

Recently, a luminescence study of Ag(I) anchored ZSM-5 zeolite at 11 K was reported [19]. The emission spectra are strongly dependent on the excitation wavelength, with each emission band becoming dominant at a characteristic excitation wavelength. Therefore, different emission bands are resolved by site-selective excitation. The luminescence results indicate that excimers as well as longer chain exciplexes are present in the Ag(I)/ZSM-5 catalyst. Experimental and theoretical results show that Ag–Ag excimers and exciplexes provide stable intermediates with NO. The increased stability of the excited state as a result of Ag–Ag bonding provides a driving force for the photodecomposition of NO into N_2 and O_2 on the surface of Ag(I)-doped ZSM-5 zeolite in catalytic sites of Ag(I) ions.

3.2. Exciplex tuning by variation of the dopant concentration

Variation of the doping level of $[Ag(CN)_2^-]$ in the host KCl crystal leads to a change in the relative intensities of the luminescence bands. To see the effect of the variation of the dopant level in the KCl host on the luminescence behavior, three mixed crystals of $Ag(CN)_2^-$/KCl (labeled as P1, P2, and P3) have been studied. Atomic absorption analysis shows that the amount of silver is 0.17, 2.7, and 4.3 wt.% for P1, P2, and P3, respectively. The three crystals were isolated from the same batch at different times during the evaporation process.

Fig. 5 shows the photoluminescence spectra of P1, P2, and P3 crystals at 77 K. As indicated in Fig. 5, band A predominates the luminescence spectra of the mixed crystal with the lowest silver content, while band C predominates the luminescence spectra of the crystal with the highest silver content. The crystal with an intermedi-

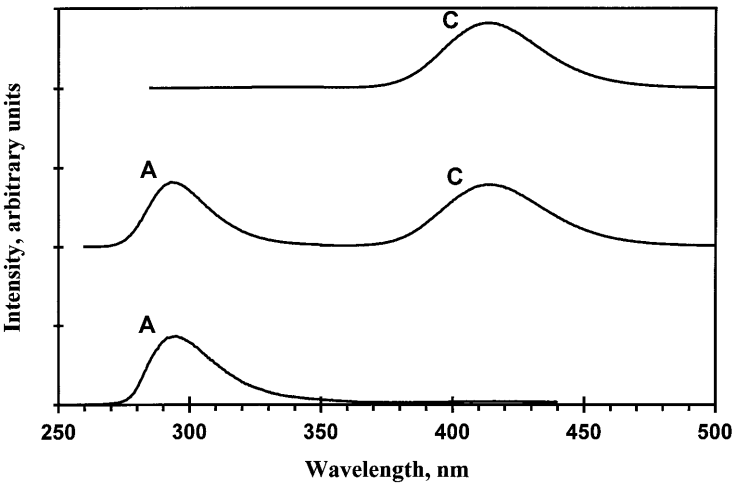

Fig. 5. Exciplex tuning by varying the dopant concentration: emission spectra of $[Ag(CN)_2^-]$/KCl crystals at 77 K. The spectra are shown for crystals with a silver content of (bottom to top): 0.17 (P1), 2.7 (P2), and 4.3% (P3). Each sample was excited with wavelengths that correspond to its most prominent excitation bands. The spectrum shown for P2 is a composite of two spectra with excitations corresponding to both bands A and C.

ate silver content has two luminescence bands A and C with almost the same intensity. The relative intensities can be explained by the extent of different Ag–Ag interactions in the three crystals. The crystal with low silver content contains mostly isolated ions or dimers of $Ag(CN)_2^-$. Since the isolated ions are not luminescent, the observed luminescence is attributed to $*[Ag(CN)_2^-]_2$. By contrast, a higher probability exists for finding trimers and longer chain oligomers in the crystals with higher silver content. Although all four bands have been observed in all three crystals, the discussion herein is restricted to bands A and C. While both bands B and C are assigned to $*[Ag(CN)_2^-]_3$ trimers, band B is not included in the analysis herein due to the strong overlap between bands B and C.

FTIR spectra of the three crystals have been studied. The spectra show multiple peaks in the υ_{CN} region. Infrared spectra of pure single crystals of $KAg(CN)_2$ show one sharp band in the υ_{CN} region [20]. This band appears at 2140 cm^{-1} and is assigned to the υ_3 fundamental mode of a $D_{\infty h}$ $[Ag(CN)_2^-]$ ion. Fig. 6 shows the infrared spectra of the $Ag(CN)_2^-$/KCl mixed crystals with high silver content P3 (Fig. 6a) and the low silver content P1 (Fig. 6b). Four resolved peaks at 2100, 2110, 2140, and 2175 cm^{-1} are distinguished (Fig. 6a) indicating the presence of several environments of $[Ag(CN)_2^-]$ ions in the mixed crystal. Fig. 6b shows a major peak at 2100 cm^{-1} with two shoulders at 2110 and 2090 cm^{-1}. This suggests that multiple C–N sites are present even in the crystal with a small silver content. The observation of peaks at high frequencies in the P3 doped crystal is attributed to the increase in the number of sites with aggregations of $Ag(CN)_2^-$ units. Consequently, silver–silver interactions increase, causing the electron density provided by the

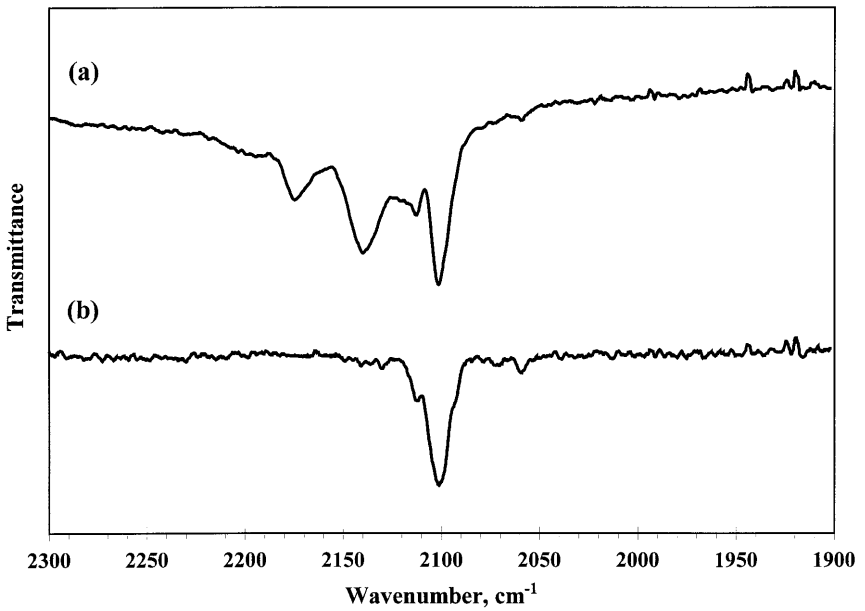

Fig. 6. Infrared spectra of single crystals of $[Ag(CN)_2^-]$/KCl in the region of the cyanide stretching frequency. The spectra are shown for single crystals with % Ag of 4.3 (a) and 0.17 (b), denoted in the text as P3 and P1, respectively.

silver to cyanide ligand to decrease. Since the LUMOs of CN^- are antibonding orbitals, the decrease in electron density from silver leads to stronger C–N bonds and higher υ_{CN}.

3.3. Energy transfer between excimers and exciplexes

In order to study the energy transfer from dimer (A sites) to trimer (C sites), time-resolved photoluminescence measurements for a $Ag(CN)_2^-$/KCl doped crystal with 2.7% Ag (crystal P2) were performed. The excitation wavelength was fixed at 250 nm.

The energy transfer processes in the crystal studied are multistep quenching pathways. The formation of stable excimers quenches any luminescence from isolated ions and results in the observation of band A. Fig. 7 illustrates that the intensity ratio of band C to band A increases when the delay time of the laser pulse is increased. This illustrates the energy transfer between $[Ag(CN)_2^-]_2$ dimer sites (band A) and $[Ag(CN)_2^-]_3$ trimer sites. To study the kinetics of the energy transfer of $Ag(CN)_2^-$/KCl, each luminescent $[Ag(CN)_2^-]_n$ oligomer in a single crystal was considered as a separate species. Scheme 1 shows the kinetic model for energy transfer processes of the various radiative and nonradiative processes in the $Ag(CN)_2^-$/KCl doped crystal labeled as P2 in this study. According to this model, excitation occurs to the $[Ag(CN)_2^-]_n$ oligomer that is responsible for band A, at a

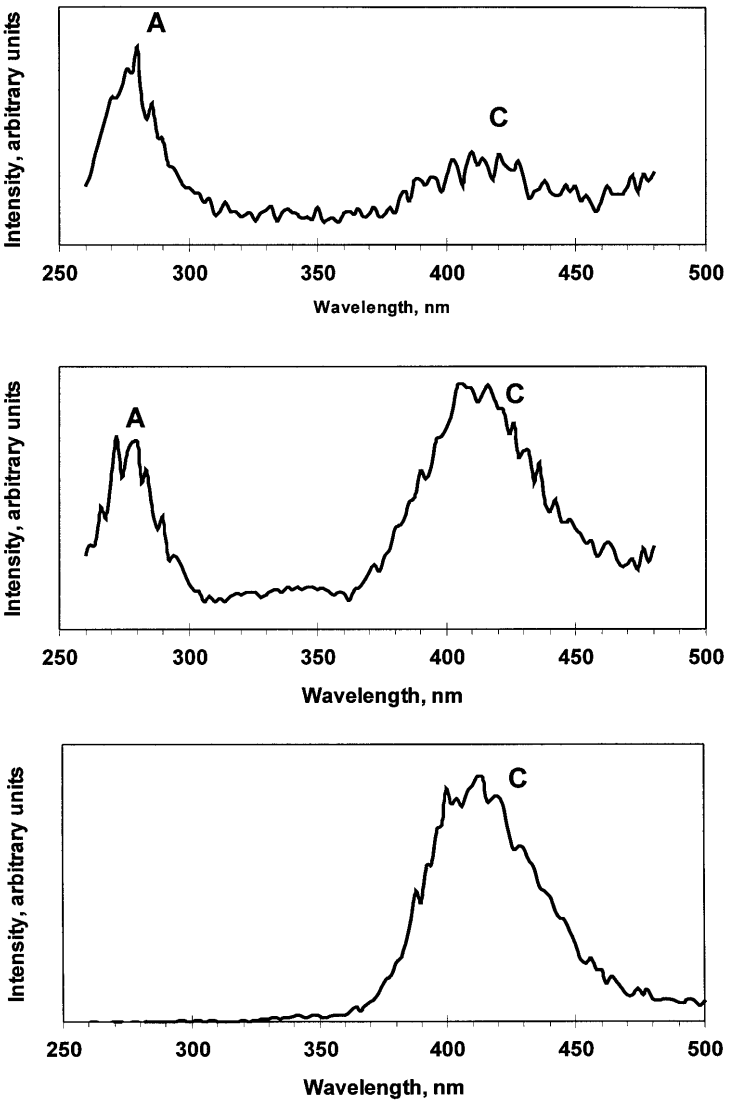

Fig. 7. Time-resolved measurements for a $[Ag(CN)_2^-]$/KCl single crystal with 2.7% Ag (P2). The excitation wavelength was selected as 250 nm in order to show energy transfer from dimer sites (band A) to trimer sites (band C). The spectra were obtained with (delay time, gate) pairs as follow: top-to-bottom (0, 5), (5, 5), and (20, 200) μs.

rate of '*w*'. The excited species can decay radiatively by emitting band A, or nonradiatively. As illustrated in Scheme 1a, the emissions from the sites responsible for bands A and C have time dependencies that can be described as follows:

$$dN_A/dt = w - k_A N_A - k_{ET} N_A - k_Q N_A \quad (1)$$

$$dN_C^{(1)}/dt = k_{ET}N_A - k_C^{(1)}N_C \quad (2)$$

Here N_A and $N_C^{(1)}$ are the population of the excitons characteristic of bands A and C, respectively. The solutions of Eqs. (1) and (2) for a δ-pulsed excitation, with the initial condition $N_C = 0$ are

$$N_A(t) = N_A(0)\exp(-\{k_A + k_{ET} + k_Q\}t) \quad (3)$$

$$N_C(t)^{(1)} = [k_{ET}/(k_C^{(1)} - k_A - k_{ET} - k_Q)]$$
$$[\exp(-\{k_A + k_{ET} + k_Q\}t) - N_A(0)\exp(-k_C^{(1)}t)] \quad (4)$$

According to Eq. (3) band A decays exponentially with only one lifetime component. Experimentally, band A has a single lifetime ($\tau_A = 2.8$ μs) obtained with $\lambda_{ex} = 250$ nm. Therefore Scheme 1a describes the time dependence of the band

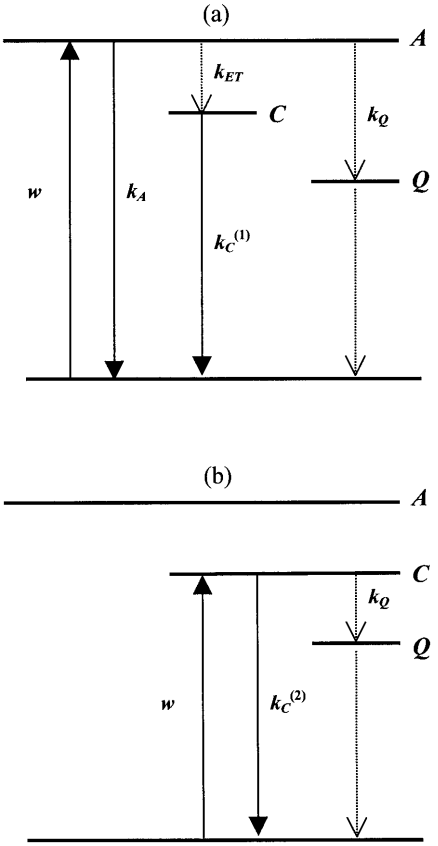

Scheme 1. Kinetic model for radiative and nonradiative processes present in $Ag(CN)_2^-$/KCl single crystals representing (a) energy transfer from band A to band C excitons, and (b) direct excitation for band C excitons.

A emission. Eq. (4) suggests that band C has a dual lifetime with a rise time and a decay time. Experimentally band C has a dual lifetime decay with a slow component $\tau_C^{(1)} = 64$ μs and a fast component $\tau_C^{(2)} = 27$ μs with virtually zero rise time. The excitation wavelength used for the lifetime data herein was 250 nm, at this wavelength the clusters responsible for band C can be excited directly. Therefore, the time dependence of band C cannot be described using Scheme 1a alone, and Scheme 1b has been used to explain the energy transfer results through the direct excitation of band C excitons. According to this mechanism, the time dependency of the dicyanoargenate(I) emission is as follows:

$$dN_A^{(2)}/dt = 0 \tag{5}$$

$$dN_C^{(2)}/dt = w - k_C^{(2)}N_C - k_Q N_C \tag{6}$$

By assuming that the rates of excitation (W) and quenching (k_Q) are the same in both mechanisms the solution of Eq. (6) will be

$$N_C(t)^{(2)} = N_C(0)\exp(-\{k_C^{(2)} + k_Q\}t) \tag{7}$$

According to Eq. (7) the band C emission by a direct excitation mechanism decays exponentially $\tau_C^{(2)} = 1/k_C^{(2)}$. Eqs. (4) and (7) show that the slow component of the band C decay lifetime (64 μs) is due to energy transfer from A while the fast component (27 μs) is due to direct excitation.

In summary, the experimental lifetime results can be explained in terms of the kinetic model shown in Scheme 1. For band A, only the mechanism shown in Scheme 1a applies, and this gives rise to a single lifetime decay (Eq. (3)), in agreement with the experimental results ($\tau_A = 2.8$ μs). Band C exhibits a rise time due to the feeding mechanism from band A and a decay time due to direct excitation. The fast component of the decay time for band C of 27 μs is significantly longer than the decay time of band A (2.8 μs). Therefore, the rate-determining step in the short-time domain for band C is direct excitation (Scheme 1b). In the long time domain, the feeding mechanism from band A is solely responsible for the band C emission, and this gives rise to the slow component in the decay time for band C (64 μs).

4. Conclusions

The role of Ag–Ag interactions appears to be significant in $KCl/Ag(CN)_2^-$ crystals as resolved by the photoluminescence measurements and molecular orbital calculations. The formation of Ag–Ag bonded excimers and exciplexes between adjacent $Ag(CN)_2^-$ ions doped in KCl gives rise to the different luminescence bands observed in the UV-Visible region of the spectra. Emission spectra can be tuned either by varying the excitation wavelengths or by changing the dopant concentration, which indicates the presence of different silver species such as monomers, dimers and trimers with different isomers.

The data suggest that bonding interactions between dicyanoargenate(I) ions occur predominantly in the lowest excited electronic state. $*[Ag(CN)_2^-]_n$ oligomers are responsible for the luminescence bands as indicated from both ab initio and Hückel calculations. Ab initio studies for aggregations of $[Ag(CN)_2^-]_n$ with $n = 2–5$ show that the HOMO has antibonding character with respect to Ag–Ag bonding, while the LUMO has Ag–Ag bonding character. Extended Hückel calculations indicate the formation of $*[Ag(CN)_2^-]_2$ excimers and $*[Ag(CN)_2^-]_3$ exciplexes. In comparison with the ground state, the Ag–Ag bond separation is shorter in the first electronic excited state, the Ag–Ag overlap population is greater in the excited state, and the potential well along the Ag–Ag bond is much deeper in the excited state. It is generally known that such ground-state interactions are absent in conventional organic exciplexes. This study indicates that this may not necessarily be the case in inorganic exciplexes because it shows the presence of ground state Ag–Ag interactions.

The independent photophysical behavior of different $[Ag(CN)_2^-]_n$ oligomers within the KCl host is illustrated by the appearance of an individual band for each oligomer. The kinetic analysis shows that excitation of a given $[Ag(CN)_2^-]_n$ oligomer can lead either to luminescence from the same oligomer or to the transfer of the excitation energy to a different oligomer. Time resolved measurements have demonstrated the existence of energy-transfer pathways between different $[Ag(CN)_2^-]_n$ oligomers.

Acknowledgements

We thank the Donors of the Petroleum Research Fund, administered by the American Chemical Society, for the support of this research.

References

[1] P.C. Ford, Coor. Chem. Rev. 132 (1994) 129.
[2] A. Edel, P.A. Marnot, J.P. Sauvage, Nouv. J. Chim. 8 (1984) 495.
[3] K.R. Kyle, P.C. Ford, J. Am. Chem. Soc. 111 (1989) 5005.
[4] K.R. Kyle, W.E. Palke, P.C. Ford, Coor. Chem. Rev. 97 (1990) 35.
[5] H. Schmidbaur, Chem. Soc. Rev. (1995) 391.
[6] F. Moser, N. Barkay, A. Levite, E. Margalit, I. Paiss, A. Sa'ar, I. Schnitzer, A. Zur, A. Katzir, Proc. SPIE 128 (1990) 1228.
[7] R.C. Baetzold, J. Phys. Chem. B 101 (1997) 8180.
[8] M.A. Omary, T.R. Webb, Z. Assefa, G.E. Shankle, H.H. Patterson, Inorg. Chem. 37 (1998) 1380.
[9] M.A. Omary, H.H. Patterson, Mol. Cryst. Liq. Cryst. 284 (1996) 399.
[10] J. Kopecky, Organic Photochemistry: A Visual Approach, VCH, New York, 1991, pp. 38–40.
[11] J. Michl, V. Bonacic-Koutecky, Electronic Aspects of Organic Photochemistry, Wiley, New York, 1990, pp. 274–286.
[12] T.H. Lowry, K. Schuller-Richardson, Mechanism and Theory in Organic Chemistry, Harper & Row, New York, 1981, pp. 919–925.

[13] C.N. Pettijohn, E.B. Jochnowitz, B. Chuong, J.K. Nagle, A. Vogler, Coor. Chem. Rev. 171 (1998) 85.
[14] M.A. Omary, H.H. Patterson, Inorg. Chem. 37 (1998) 1060.
[15] M.A. Omary, H.H. Patterson, J. Am. Chem. Soc. 120 (1998) 7696.
[16] M.A. Omary, D.R. Hall, G.E. Shankle, A. Siemiarczuk, H.H. Patterson, J. Phys. Chem. B 103 (1999) 3845.
[17] M. Rawashdeh-Omary, M.A. Omary, G.E. Shankle, H.H. Patterson, J. Phys. Chem. B (1999) submitted.
[18] W.R. Mason, J. Am. Chem. Soc. 95 (1973) 3573.
[19] S.M. Kanan, M.A. Omary, H.H. Patterson, M. Matsuoka, M. Anpo, J. Phys. Chem. B. (2000) in press.
[20] L.H. Jones, J. Chem. Phys. 26 (1957) 1578.